Signal and Image Processing Letters
Vol. 5., No. 1, 2023, pp. 48-61
ISSN 2714-6677
https://simple.ascee.org/

Numerical simulation of highly efficient Cs_2TiI_6 based Cd free perovskites solar cell with the help of optimized ETL and HTL using SCAPS-1D software

Md. Abdul Halim [a,1,*], Md. Shafiqul Islam [a,2], Md. Momin Hossain [b,3], Md. Yakub Ali Khan [b,4]

[a] Department of Electrical and Electronic Engineering, Prime University, Mirpur-1, Dhaka-1216, Bangladesh
[b] Department of Electrical and Electronic Engineering, World University of Bangladesh, Uttara, Dhaka-1230, Bangladesh
[1] halimabdul552@gmail.com; [2] shuvo5684@gmail.com; [3] hmomin89@gmail.com; [4] yakub.bimt@gmail.com
* corresponding author

ARTICLE INFO

Keywords
erovskite Solar Cell
Optimization
Solar Cell Capacitance
lead-free perovskite
Cs_2TiI_6

ABSTRACT

In order to provide the best photovoltaic application, this paper examines the physical, optical, and electrical aspects of Cesium Titanium (IV) based single halide Perovskite absorption materials. Perovskite solar cell for scavenging renewable energy, has grown more and more necessary in the context of the diversification of the use of natural resources. Due to its efficient band gap of 1.8 eV, Cs_2TiI_6 has become a desirable contender for today's thin-film solar cell. This article shows the spectrum responses of a planar Au/FTO/C60/Cs_2TiI_6/$CH_3NH_3SnI_3$/Al based structure where $CH_3NH_3SnI_3$ is used as a Hole transport layer (HTL) and C60 and FTO are utilized as Electron transport layers (ETL) under 300K temperature conditions. This research demonstrates that employing Fluorine doped Tin Oxide (FTO) and Ultrathin Fullerene (C60) as Electron transport layer charge extraction can be achieved. FTO provides high transmission, strong conductivity, and good adherence for the deposited layers. When used in a coevaporated perovskite solar cell, a C60 layer with an ideal thickness less than 15 nm improves charge extraction. This article tried to avoid cadmium for solar cell generation due to its toxicity on environment. The simulation included detailed configuration optimization for the thickness of the absorber layer, HTL, ETL, defect density, Wavelength, temperature, and series resistance. In this work the Power Conversion Efficiency (η), Fill Factor (FF), Open-circuit Voltage (Voc), J-V Curve, Quantum Efficiency and Short-circuit current (Jsc) have been measured by varying thickness of absorber layer in the range of 1µm to 6 µm. Energy harvesting effectiveness, cost-effectiveness of perovskite solar cells is all impacted by their PCE, which is a crucial characteristic. The key variables that define a perovskite solar cell's performance are the Voc and fill factor (FF). When the voltage is zero, the solar cell can produce its maximum current, which is represented by the (Isc). The optimized perovskite solar cell shows a power conversion efficiency of 21.8429% when the absorber layer thickness is 4µm and electron transport layer thickness is 0.6µm.

1. Introduction

In today's world, there is a demand for a sustainable, renewable, economical, and clean energy to address the main challenges of global warming. Examples of renewable energy sources include wind, geothermal, bio, solar energy, and hydropower and mechanical vibration [1]

Among these renewable sources solar is tremendously growing its research interest due to abundancy. There are many types of solar cell on which researchers are doing work for example Si-based solar cell, thin film solar cell and perovskite solar cell. Perovskite solar cells are designed to boost solar energy efficiency and cut costs. In fact, perovskite photovoltaics show potential in terms of high efficiency, relatively low material prices, and low operating costs. For making perovskite solar cell it is very important to select proper materials.

In particular, cadmium telluride (CdTe) thin-film solar cells are made using cadmium (Cd), which is frequently employed in the fabrication of solar cells. Here are a few explanations for why it's so popular. Optimal Bandgap, High Absorption Coefficient, Abundance and Low Cost, High Conversion Efficiency are the key factor for using Cd. However, Cd has bad impact on environment such as soil contamination, toxicity to organisms, human health risk and water pollution. For the above mentioned problems author tried to avoid Cd in this research. Materials play a key role in the creation of highly efficient solar cells. Researchers have discovered a few solar energy materials with excellent light absorption and sufficient physical characteristics to raise solar cell efficiency. Materials like SnS [2], Cu_2O [3], Cu_2SnS_3 [4], Cu_2GeS_3 [5], $GeSe$ [6], Sb_2S_3 [7], Sb_2Se_3 [8], and others have been investigated for use in solar cells for thin film.

Due to its photovoltaic characteristics, perovskite solar cells (PSC) have experienced considerable growth over the past few years. It has sparked intense curiosity among researchers in regards to its photovoltaic use. To further examine the performance of solar cells, researchers have proposed various Perovskite materials with various cell architectures. Despite these advancements in the next generation of solar cells, stability continues to be a major obstacle to industrial application and commercialization. When the first thin film-based third generation Perovskite solar cells were created, they contained an organic-inorganic compound with the chemical formula ABX_3, where X is an anion and may be one of the halide elements Br, I, Cl, or F, and A and B are cations [9]. Anion position has a significant impact on how energy is produced. This type of hybrid organic-inorganic halide PSC is most suited to serve as a photo active layer due to its several benefits, including increased light absorption, charge carrier mobility, higher exciton diffusion length, reduced exciton binding energy, and tunable band gap. In turn, this leads to increased power conversion efficiency (PCE, %). Kojima was the first to introduce such a hybrid halide with $CH_3NH_3PbI_3$ and $CH_3NH_3PbBr_3$ as the active components for solar cells, and PCE was up to 3.8% [9].

The PCE was then improved by 9.7% when the researcher employed organic spiro MeOTAD as the solar cell's Hole transfer material [10]. More thorough investigation into the $CH_3NH_3PbI_3$ solar cell yielded the best conversion efficiency >20%, which is more than any conventional dye-sensitized solar cell (DSSCs) [11]. As an alternative to indium-doped tin oxide (ITO), fluorine-doped tin oxide (FTO) electrodes have been researched. ITO sheet resistance, however, will rise with heating, resulting in a higher series resistance in the finished product. It is demonstrated that FTO has a number of advantages over ITO, including cost [12]. There are many compound materials for example Cs_2TiBr_6, $Cs_2TiI_1Br_5$, $Cs_2TiI_2Br_4$, $Cs_2TiI_3Br_3$, $Cs_2TiI_4Br_2$, $Cs_2TiI_5Br_1$, and Cs_2TiI_6 which are used in perovskite solar cell currently [13]. In the current study, two distinct ETL (FTO and C60) has been used with an alternative structure of Cs_2TiI_6 based absorbing material to determine the quantum efficiency [14].

For effective charge transport to and extraction from the perovskite absorber layer in perovskite solar cells, the optimized electron transport layer (ETL) and hole transport layer (HTL) are key components. The ETL is typically located between the perovskite absorber layer and the electron-collecting electrode (e.g., a transparent conducting oxide like fluorine-doped tin oxide). The primary purpose of the ETL is to efficiently transport the photo-generated electrons from the perovskite layer to the electron-collecting electrode. Typically, the HTL is positioned between the hole-collecting electrode (such as a conductive polymer or metal) and the perovskite absorber layer. From the perovskite layer to the hole-collecting electrode, photo-generated holes need to be extracted and transported, and the HTL makes this easier.

Perovskite solar cells that have been optimized have the potential for many real-world uses because of their special qualities and advantages. Here are a few possible uses for improved perovskite solar cells in real life, including building-integrated photovoltaics (BIPV), porTable and wearable devices, off-grid power generation, consumer electronics, transportation, large-scale solar power plants, and emerging applications. In addition, perovskite solar cells are being investigated for new uses such

indoor solar cells (harvesting indoor lighting), transparent solar cells (integrating into windows without obscuring views), and solar-driven water splitting for hydrogen production. It's crucial to keep in mind that even though perovskite solar cells have a lot of potential, there are still obstacles to be solved. For example, their long-term stability, toughness, and production processes need to be scaled up. Nevertheless, efforts are still being made in research and development to overcome these obstacles and realize the full potential of perovskite solar cells in a variety of applications.

Due to the benefits they provide over other types of solar cells, perovskite solar cells have attracted a lot of attention and research interest in recent years. Perovskite solar cells have outperformed several other types of solar cells in terms of their power conversion efficiencies (PCEs). Perovskite solar cells now have a record PCE of over 25%, which is comparable to conventional silicon-based solar cells. The field of perovskite solar cells is advancing rapidly, with frequent breakthroughs and improvements in efficiency and stability. Perovskite solar cells can be fabricated as thin and lightweight films, making them suiTable for flexible and porTable applications.

The goal of Perovskite thin film solar cells is increasingly helping to close the gap in power supply in remote places without connection to the grid. The perovskite solar cell revolution has created numerous new business opportunities for the leading energy firms. The goal of this study is to help the researcher increase the amount of perovskite solar-cell-based energy that can be utilized to replace fossil fuels as a long-term solution for both the environment and the economy.

2. Method

The SCAPS-1D Version 3.3.10 simulator software screen has been used to reset the simulation process, which was run under 300 K ambient temperature, 1.5 AM light illumination, and 1000 W/m2 power [15]. The working process of SCAPS for this perovskite solar cell is shown in Fig. 1 [16]. A Cs_2TiI_6 based perovskite solar cell consisting of six layers has been shown in Fig.2. In Fig. 2 Schematic view of proposed perovskite solar cell has been modeled. Here, both ETL has higher band gap which is 3.5 eV for FTO and 1.7 eV for $C60$. The given structure of Fig. 2 shows a 6-layers structure and further it can be extended up to 7 layers as per the device structure if needed.

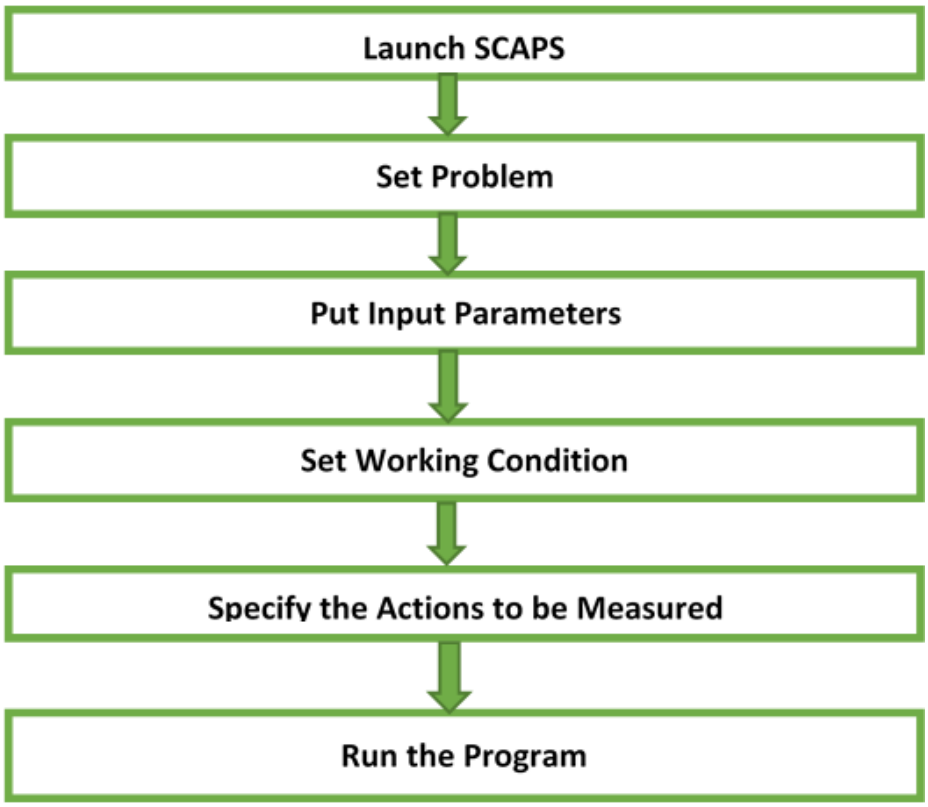

Fig. 1. Simulation procedure for SCAPS-1D

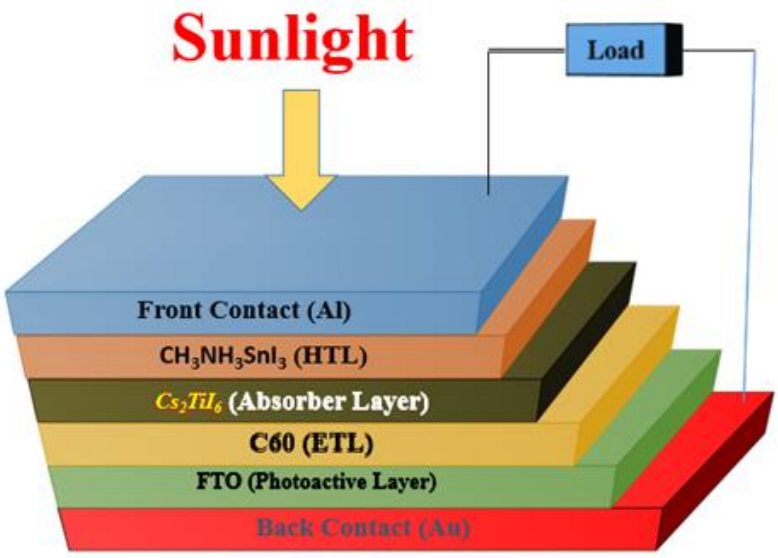

Fig. 2. Schematic diagram of Cs_2TiI_6 based solar cell

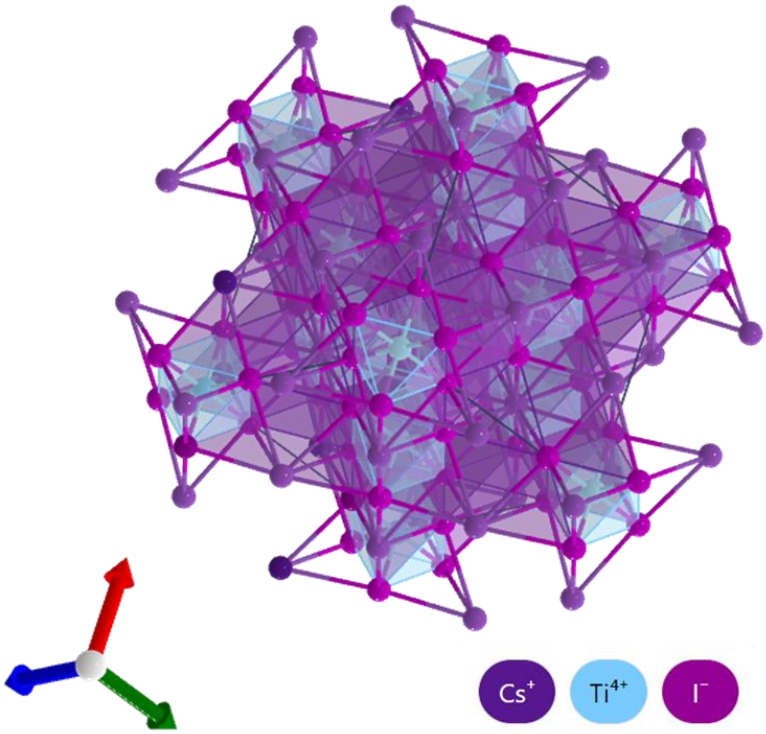

Fig. 3. Crystal structure of Cs_2TiI_6

The lattice parameter of Cs_2TiI_6 crystal structure a= 11.86 Ao, b= 11.86 Ao, c= 11.86 Ao and angle $\alpha = \beta = \gamma = 90°$

Cs_2TiI_6 crystallizes in the cubic $Fm\bar{3}m$ space group shown in Fig. 3. Cs^{1+} is bonded to twelve equivalent I^{1-} atoms to form CsI_{12} cuboctahedra that share corners with twelve equivalent CsI_{12} cuboctahedra, faces with six equivalent CsI_{12} cuboctahedra, and faces with four equivalent TiI_6 octahedra. All $Cs-I$ bond lengths are 4.20 Å. Ti^{4+} is bonded to six equivalent I^{1-} atoms to form TiI_6 octahedra that share faces with eight equivalent CsI_{12} cuboctahedra. All $Ti-I$ bond lengths are 2.78 Å. I^{1-} is bonded in a distorted single-bond geometry to four equivalent Cs^{1+} and one Ti^{4+} atom.

V-I characteristics, Quantum Efficiency (QE), Power Conversion Efficiency (PCE), Fill Factor(FF), Open Circuit Voltage (VOC) and Current Density (JSC) has been measured from structure

in Fig. 2. Data has been taken frequently by varying thickness of various layer and then found optimal device. The optimal device has given maximum quantum efficiency in the range 360 nm to 680 nm.

There are a number of restrictions to take into account, even if simulation methods like SCAPS-1D (Solar Cell Capacitance Simulator in 1 Dimension) can offer useful insights into the performance and behavior of perovskite solar cells. For the purpose of describing the behavior of the various layers and interfaces in a perovskite solar cell, SCAPS-1D uses simple mathematical models and assumptions. These simulations and experiments might not accurately reflect all the intricate physical events and processes that take place in real devices. The accuracy of the simulation can be impacted by inaccurate or vague material attributes. The sensitivity of SCAPS-1D simulations to changes in input parameters can vary. The significance of precisely selecting input values is highlighted by the fact that sometimes even minor changes in a device's specifications or a material's characteristics can result in noticeable alterations in the simulated device's performance.

This simulation-based work evaluated the Fill Factor of 74.1557%, Open-circuit Voltage of 1.043057 V, and Current Density of 28.23949898 A and discovered a maximum efficiency of better than 21.84% for an optimized perovskite solar cell when the absorber layer thickness is 4 µm.

In this case, Table 1 shows the characteristics of the basic material, and Table 2 shows the characteristics of the absorbing material [17].

Table 1. The parameters for the Cs_2TiI_6 based solar cell at 300K

Parameters	Cs_2TiI_6	$CH_3NH_3SnI_3$ (HTL)	C60 (ETL)	FTO
E_g(eV)	1.8	1.3	1.7	3.5
ε_r	5	6.5	4.2	9
χ(eV)	4.2	3.9	3.9	4
µn($cm^2V^{-1}S^{-1}$)	4.4	1.6	8.0×10^{-2}	2.0×10^{1}
µp($cm^2V^{-1}S^{-1}$)	2.5	1.6	3.5×10^{-3}	1.0×10^{1}
N_D (cm^{-3})	1.9×10^{19}	0	1.0×10^{18}	1×10^{18}
N_A (cm^{-3})	1.0×10^{19}	3.2×10^{18}	0	0
V_t(cm/s)	1×10^{7}	1×10^{6}	1×10^{7}	1×10^{7}
V_t(cm/s)	1×10^{7}	1×10^{6}	1×10^{1}	1×10^{7}

Table 2. Properties of absorbing materials [18]

Properties	Cs_2TiBr_6	$Cs_2TiI_1Br_5$	$Cs_2TiI_2Br_4$	$Cs_2TiI_3Br_3$	$Cs_2TiI_4Br_2$	$Cs_2TiI_5Br_1$	Cs_2TiI_6
Thickness (nm)	750	750	750	750	750	750	750
Band gap, Eg (eV)	1.78	1.58	1.38	1.26	1.15	1.07	1.8
Electron affinity, Ea (eV)	3.22	3.42	3.62	3.74	3.85	3.93	4.2
Relative Permittivity, Ɛr	3.75-5.06	3.75-5.06	3.75-5.06	3.75-5.06	3.75-5.06	3.75-5.06	5
Donor density, ND ($1/cm^3$)	1.0×10^{19}	1.0×10^{19}	1.0×10^{19}	1.0×10^{19}	1.0×10^{19}	1.0×10^{19}	1.9×10^{19}
Acceptor density, NA($1/cm^3$)	1.0×10^{19}	1.0×10^{19}	1.0×10^{19}	1.0×10^{19}	1.0×10^{19}	1.0×10^{19}	1.0×10^{19}
Electron mobility, µn (cm^2 /VS)	4.4	4.4	4.4	4.4	4.4	4.4	4.4
Hole mobility, µp (cm^2 /VS)	2.5	2.5	2.5	2.5	2.5	2.5	2.5

3. Result and Discussion

The main objective of this thesis is to see how changing thickness of various layer affect the light conversion efficiency of Cs_2TiI_6 based perovskite solar cells. The use of the optimized data will allow us to establish a set of criteria for real-time solar photovoltaic device design with the highest power

conversion efficiency PCE). This in-depth investigation allowed us to measure the QE(η), PCE (η), Fill Factor (%), Open-circuit Voltage (Voc) and Short-circuit current (Jsc) in the Cs_2TiI_6 based thin film solar cell, allowing the research community to develop more efficient solar cell devices. In this paper Au/FTO/C60/Cs_2TiI_6/$CH_3NH_3SnI_3$/Al perovskite solar cell has been investigated and we found the efficiency 21.8429% as shown in Table 3.

The impact of temperature on perovskite solar cell has been discussed in this paper. The efficiency of a solar cell device is influenced by temperature. Testing temperatures are normally 300°K, even though a solar cell device's operational temperature is typically higher than that. The ideal temperature of the simulated model is modified to 300K in order to attain great efficiency. The model has a maximum efficiency of 21.8429 percent, a fill factor of 74.1557 percent, a Jsc of 28.23949898 mA/cm2, and a Voc of 1.043057 V at this temperature. It's crucial to remember that the precise impacts of temperature on perovskite solar cells can differ based on elements including device architecture, materials, and particular operating conditions. Additionally, research is being done to create ways, such as the use of sophisticated materials and encapsulating methods, to reduce the detrimental effects of temperature and improve the thermal stability of perovskite solar cells.

As a result of this investigation, it is evident that for considerably thicker absorbing layers of Cs_2TiI_6 after 4 µm, the values of the VOC, JSC, and PCE do not vary appreciably because at the greater thicknesses, the incoming photons are thoroughly absorbed by the absorbent material. Due to the electron-hole pair's inability to enter the space charge area like a result of the increase in charge carrier diffusion length, the rate of bulk recombination is accelerated. As a result, 4 µm will be taken into account as the optimal thickness for the Cs_2TiI_6 absorbent layer.

Table 3. Perovskite parameters for the Cs_2TiI_6 based solar cell

Device Structure	Open circuit Voltage VOC(V)	Current Density JSC (mA/cm²)	Fill Factor FF (%)	Power Conversion Efficiency η (%)
Au/FTO/C60/Cs_2TiI_6/$CH_3NH_3SnI_3$/Al	1.043057	28.23949898	74.1557	21.8429

A comparison of Power Conversion Efficiency, Fill Factor, Open Circuit Voltage, and Current Density for the present device performance with the other existing work has been given in Table 4.

Table 4. Comparison with related work

Device Structure	Open circuit Voltage Voc(V)	Current Density Jsc (mA/cm²)	Fill Factor FF (%)	Power Conversion Efficiency η (%)	Reference
Cs_2TiBr_6	0.89	3.87	59.5	2.15	[19]
Cs_2TiBr_6	1.53	8.66	86.45	11.49	[20]
Cs_2TiBr_6	1.12	10.25	73.59	8.51	[21]
Cs_2TiI_6	1.74	22.74	41	16.31	[22]
Cs_2TiI_6	1.95	17.19	38	12.73	[22]
Cs_2TiI_6	1.043057	28.23949898	74.1557	21.8429	Present Work

3.1. Effect of Absorber Layer's Thickness variation on PCE, JSC, FF and VOC at 300 K Temperature

In this section, the physical parameters of the halide-based absorbing material Cs_2TiI_6, including the absorbing layer thickness, device temperature, and defect density, have been numerically optimized using the SCAPS-1D simulator at the 300 K device temperature with a typical 10^{10} cm^{-3} defect density.

Fig. 4 displays the thickness graphs for absorbing materials for open circuit voltage (VOC), short circuit current (JSC), Power Conversion Efficiency (PCE), and fill factor (FF). The recombination of electron and hole pairs is discovered to be improved for thicker absorbent layers. Following that thickness, PCE begins to decline sharply. As a result of this investigation, it is evident that for

considerably thicker absorbing layers than 4 µm Cs_2TiI_6, the values of the VOC, JSC, FF and PCE do not vary appreciably because at these thicker layers, incoming photons are thoroughly absorbed by the absorbent material. The electron-hole pair is unable to reach the space charge area as a result, increasing the bulk recombination process.

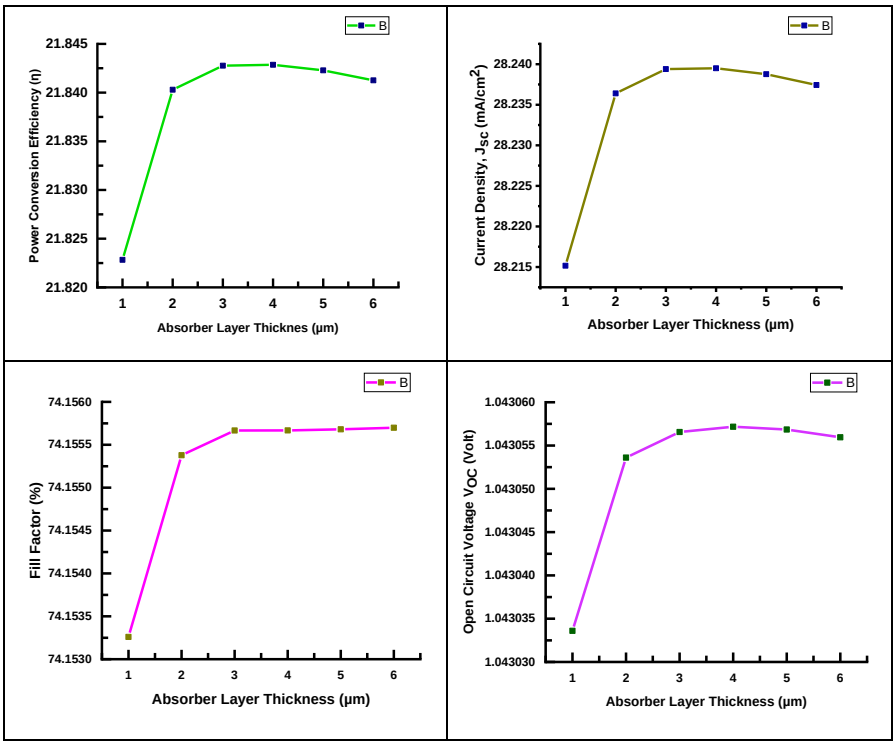

Fig. 4. Effect of absorber layer thickness variation on PCE, JSC, FF and VOC at 300 K temperature

This is because the diffusion length of the charge carrier has increased so considerably. As a result, 4 µm will be taken into account as the optimal thickness for the Cs_2TiI_6 absorbent layer [23]. This author attempted to take values of different parameters by changing the values of thickness of absorber layer in the range from 1 µm to 6 µm. In this paper Power Conversion Efficiency 21.8429 %, Fill Factor 74.1557 %, Open-circuit Voltage 1.043057 V and Short-circuit current 28.23949898 mA/cm^2 when the absorber layer thickness is optimized as 4µm.

3.2. Effect of Defect Density on Efficiency, Current Density, Open Circuit Voltage and Fill Factor for Absorber Layer Thickness

Another important factor that directly affects the performance metrics of solar cells is defect density. The majority of the photo generated current is produced by the absorber layer. Therefore, an increase in carrier recombination results from an increase in defect density, which in turn impacts the device efficiency. This work varies the defect density between 10^{10} cm^{-3} and 10^{18} cm^{-3} in order to evaluate the impact of the defect density. It is demonstrated that the defect density significantly affects the perovskite solar cell's output parameter in Fig. 5.

As seen in Fig. 5, the PCE of the Cs_2TiI_6 perovskite solar cell begins to decline as the defect density rises over 10^{10} cm^{-3}. The values of defect density published in [24] are in good agreement with the values discovered during the simulation. As depicted in Fig. 5, the open circuit voltage and short circuit current for Cs_2TiI_6 decrease with large values of (>10^{10} cm^{-3}) for defect density. Along with an increase in defect density, the fill factor value likewise falls but after 10^{12} cm^{-3} before 10^{12} cm^{-3}. Increases in carrier recombination rate and defect density lead to a reduction in carrier lifespan and diffusion length. Consequently, the device's overall performance suffers [25]. In [26] author reported defect density values that are in good agreement with the values found during the simulation. As depicted in Fig. 5, the open circuit voltage and short circuit current for Cs_2TiI_6 decrease with large values of defect density. Along with an increase in defect density, the fill factor value likewise falls. The carrier lifetime and diffusion length decrease as the defect density and carrier recombination rate both rise. As a result, the device's overall performance declines [27].

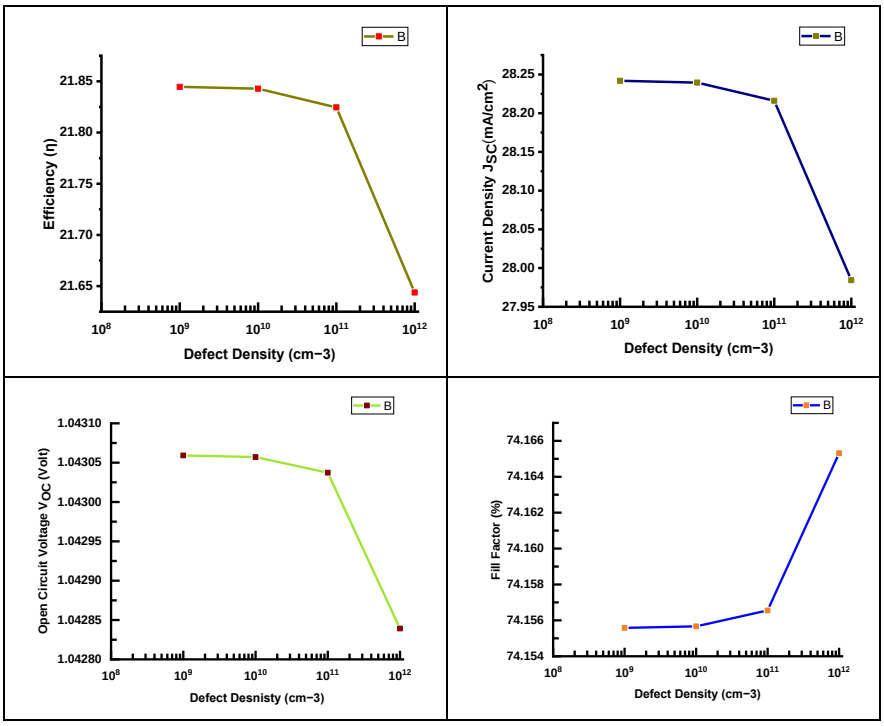

Fig. 5. Effect of defect density on efficiency, current density, open circuit voltage and fill factor for absorber layer thickness

3.3. Effect of ETL on Cs_2TiI_6 Absorber Layer Based Solar Cell

We suggest ETMs for inquiry in this part in order to produce high performance of PSCs, VOC, JSC and FF. In Fig. 6, the effect of Electron Transport Layer on Cs_2TiI_6 absorber layer based thin film perovskite solar cell C60 as ETM has been shown. The thickness of ETL has been checked in the range from 0.6 um to 1 um. The impact of ETM layer thickness on the characteristics of perovskite solar cells is illustrated in Fig.6. According to the data, as thickness increases from 0.6 to 1 um, efficiency slightly from 21.84% to 22.02 %.

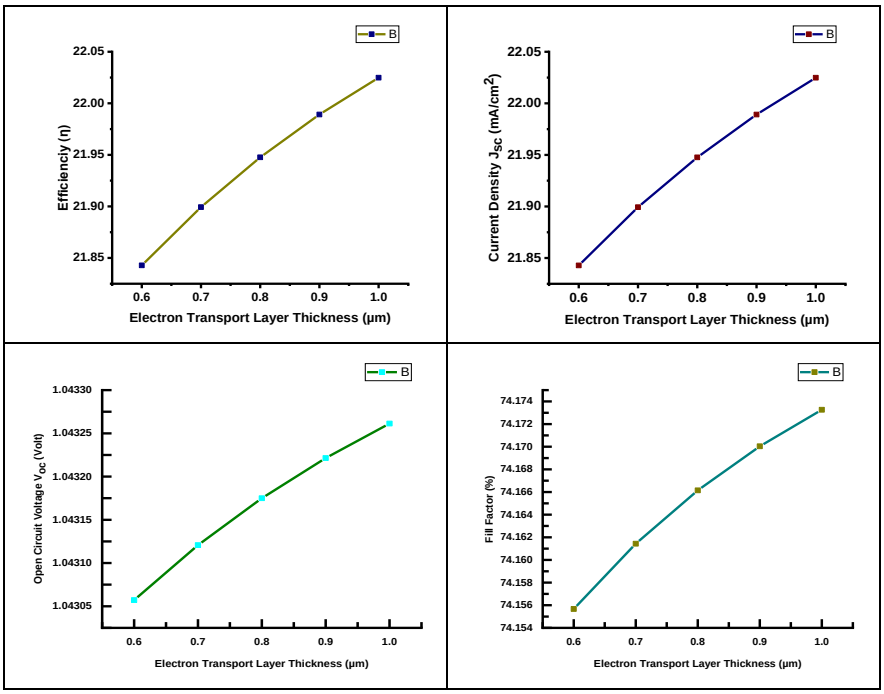

Fig. 6. Effect of ETL on PCE, JSC, VOC and FF

Likewise, efficiency, current density, open circuit voltage and fill factor slightly changed from 28.23 mA/cm^2 to 28.46 mA/cm^2, 1.04 V to 1.04 V and 74.15% to 74.17% respectively [28]. This demonstrates that the electrical characteristics of the perovskite solar cell are not significantly influenced by the electron transport layer. Perovskite solar cells with a planar structure have only recently been developed. This is explained by the fact that the ETM layer is merely a charge transport layer and that the perovskite material itself could assist in the creation of charge carriers via photon excitation.

3.4. Effect of HTL on Cs_2TiI_6 Absorber Layer Based Solar Cell

To achieve high performance of PSCs, VOC, JSC, and FF, we propose HTMs for investigation in this section. The thin film perovskite solar cell $CH_3NH_3SnI_3$ with a Cs_2TiI_6 absorber layer based Hole Transport Layer effect is presented in Fig. 7. HTL has been tested in the thickness range of 0.1 um to .5 um.

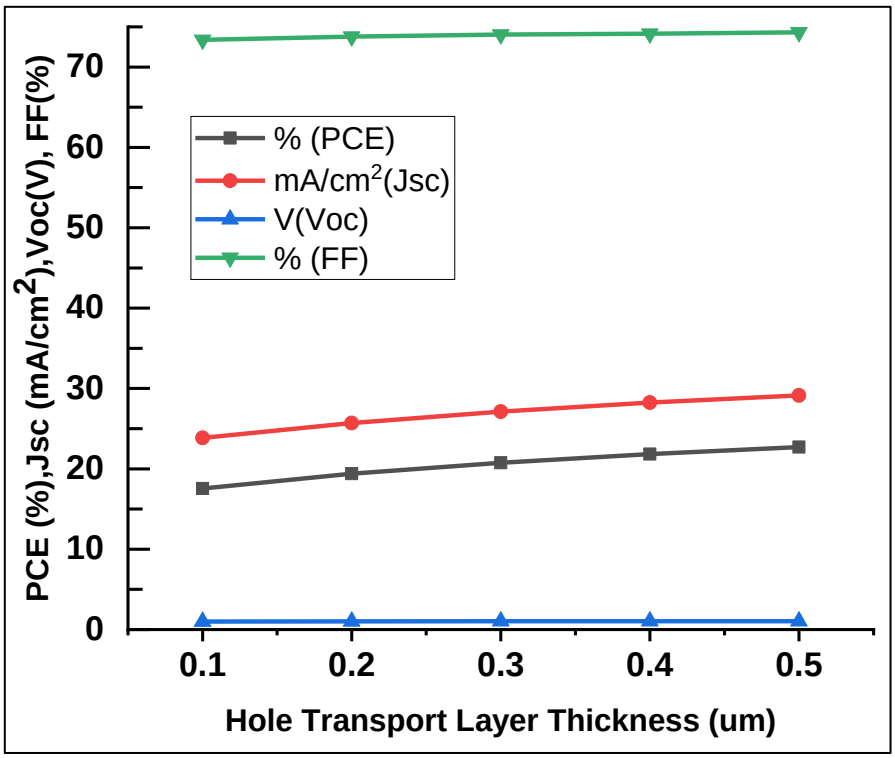

Fig. 7. Effect of HTL on PCE, JSC, VOC and FF

Fig. 7 shows how the thickness of the HTM layer affects the traits of perovskite solar cells. The findings show that efficiency increases from 17.55% to 22.71% when thickness increases from 0.1 um to .5 um. Similar to efficiency, current density, open circuit voltage, and fill factor, which went from 23.86 mA/cm^2 to 29.13 mA/cm^2, 1.0 V to 1.05 V, and 73.38% to 74.32%, respectively, marginally changed. This shows that as the thickness is increased, the electrical properties of perovskite solar cells like PCE and JSC increase. However, there is no discernible change at all in VOC and FF.

3.5. Effect Wavelength on Quantum Efficiency

The illumination of light was studied for all Perovskite materials in Fig.8 from 200 to 1000 nm wavelength, and it reveals that Cs_2TiI_6 active materials are active up to 660 nm wavelength. Between 350 nm and 660 nm, the device may operate at 100% quantum efficiency before steadily declining beyond that [29].

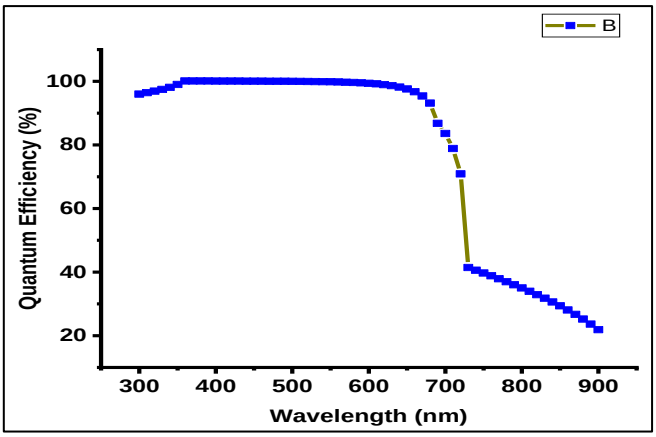

Fig. 8. Output waveform quantum efficiency for optimized wavelength

The mathematical equation of the quantum efficiency is defined as in Equation 1 [30] Where e is the electron's charge (1.6 10^{-19} C), Iph is the number of electrons (holes) collected each second, h is the Planck's constant (6.62 10^{-34}) and P is the incident optical power (Watt).

$$QE(\%) = \frac{h\gamma I_{ph}}{eP}$$

From Fig.8, it is obvious that QE for the Cs_2TiI_6 active materials has begun to steadily decline after he 660 nm wavelength. This large drop shows a reduction in light absorption by the absorbent materials as a result of enhanced light reflection.

3.6. Effect of Temperature Effect on Cs_2TiI_6 Based Perovskite Solar Cell

According to Fig. 9, when the absorber layer thickness is 4.0 μm, the impact of operation temperature on the photovoltaic performance of the proposed Ld-free Cs_2TiI_6-based Perovskite Solar Cell is investigated. The working temperature of the Ld-free Cs_2TiI_6 -based Perovskite Solar Cell has been raised from 270K to 470K in order to attain stability. Voc fell sharply from 1.04 V to 1.02 V when operational temperature rose. As the temperature rose, Jsc little changed, as seen in Fig. 9.

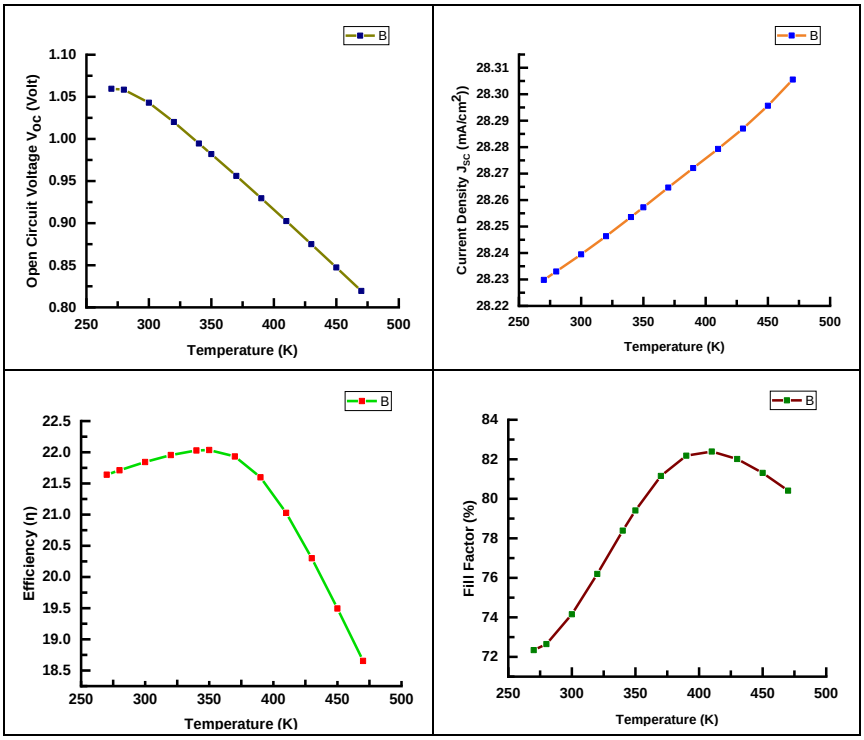

Fig. 9. Effect of temperature of on PCE, JSC, VOC and FF for Cs_2TiI_6 based Perovskite Solar Cell

When the temperature rose from 280 K to 300 K and continued until 430 K, the fill factor climbed from 72.64% to 74.15%. However, at 430 K, the fill factor started to decline. Maximum Efficiency of 21.84% is discovered for an optimal device at temperature 300K and tends to rise till 370K after PCE has declined from 370K to 470K, as illustrated in Fig. 9. Temperature has an impact on how well a solar cell device works. Although a solar cell device's operational temperature is typically higher than 300°K, testing temperatures are typically 300°K [31]. Series resistance increases as diffusion length shortens, reducing fill factor and efficiency [32]. To achieve high efficiency, the ideal temperature of the simulated model is changed to 300K. At this temperature, the model's maximum efficiency is 21.8429 percent, with a fill factor of 74.1557 percent, JSC equal to 28.23949898 mA/cm^2, and VOC equal to 1.043057 V.

3.7. Effect of Resistance on Cs_2TiI_6 Based Perovskite Solar Cell

The technologies used in perovskite solar cells are impacted by series resistance (Rs). The front- and back-surface metallic contacts' resistance, the bulk resistance, as well as additional circuit resistances from terminals and connections, all contribute to the series resistance. The shunt resistance is brought on by leakage currents. Partial junction shorting, especially towards the cell boundaries, is caused by non-idealities and impurities close to the pn junction [33]. To obtain high power conversion efficiency, it is preferable to obtain low series and high shunt resistances. JSC and VOC are both impacted. A flawless FF is impossible to accomplish. Even if we are able to get a zero series resistance (Rs) and an endlessly huge shunt resistance (Rsh), this is due to the solar cell's problematic diode behavior [34]. The effect of RS on photovoltaic parameters like VOC, JSC, FF, and power conversion efficiency was evaluated using the SCAPS-1D simulator. The shunt resistance was maintained while changing the series resistance from 1 Ω to 8 Ω. The open circuit voltage and current density, as illustrated in Fig. 10, hardly alter as series resistance increases. But the increase in series resistance has resulted in a shift in the Fill Factor, which went from 71.66% to 54.70%. The rise in series resistance RS has caused the conversion efficiency, which was 21.15%, to drop to 16.1%.

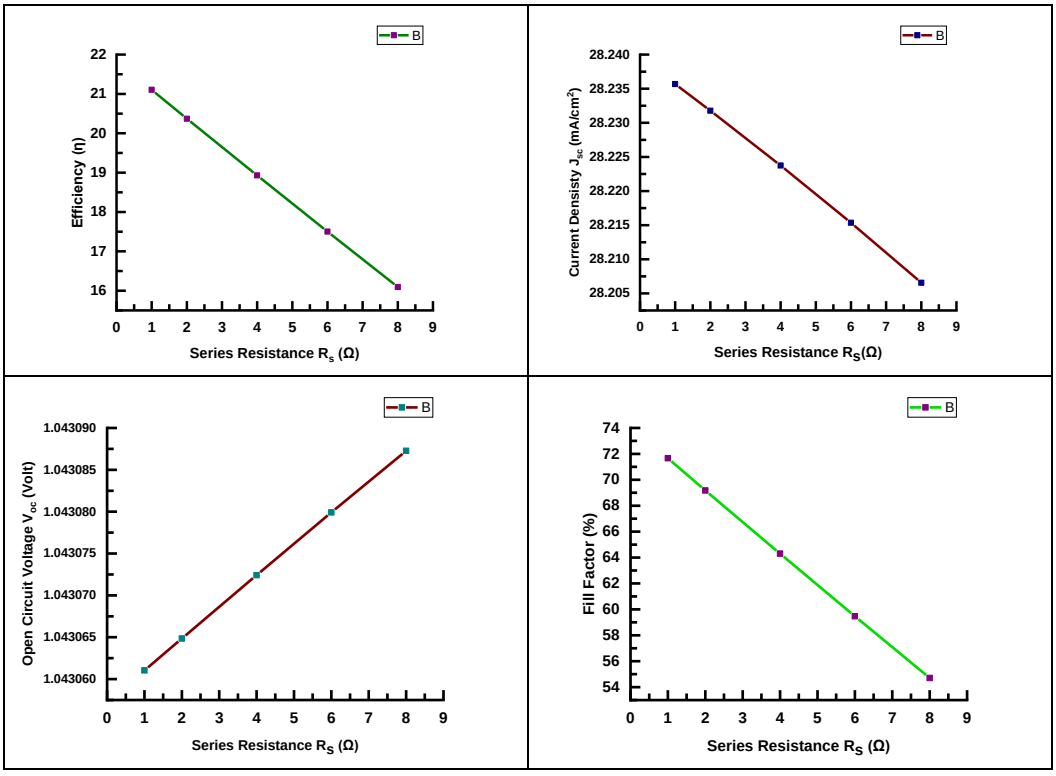

Fig. 10. Effect of Resistance of on PCE, JSC, VOC and FF for Cs_2TiI_6 Based Perovskite Solar Cell

3.8. J-V Characteristics Curves of Cs_2TiI_6 Based Perovskite Solar Cell

A perovskite Cs_2TiI_6. Based solar cell's predicted J-V characteristics are shown in Fig.11. The four photovoltaic parameters of a Cs_2TiI_6 based perovskite solar cell PCE, JSC, VOC and FF has been found from this J-V characteristics curve. According to the diagram, perovskite solar cells containing

Cs_2TiI_6 as an observer C60 and FTO as Electron Transport Layer (ETL) and $CH_3NH_3SnI_3$ as a Hole Transport Layer (HTL) have high conversion efficiency. The maximum efficiency obtained is 21.8429 % for Cs_2TiI_6 as an observer layer for perovskite thin film solar cell. At this characterization of Cs_2TiI_6 based thin film perovskite solar cell it is found PCE equal to 21.8429 %, FF equal to 74.1557 %, VOC equal to 1.043057 V and JSC equal to 28.23949898 mA/cm^2 at absorber layer thickness of 4µm.

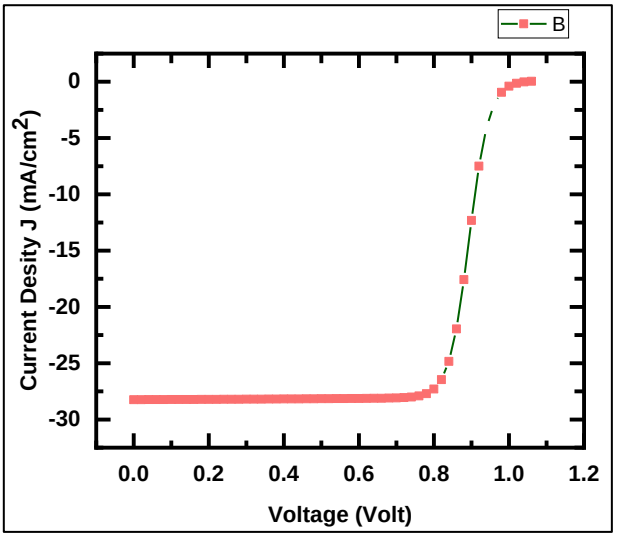

Fig. 11. J-V characteristics curve of Cs_2TiI_6 based solar cell

4. CONCLUSION

The suggested Cs_2TiI_6 based perovskite thin film solar cell structure is optimized for thickness, device temperature, Resistance effect and defect density in terms of J-V, PCE, FF, Q-E, V_{OC} among other performance characteristics. At a thickness of 4 µm, a device temperature of 300 K, and a defect density of 10^{10} cm^{-3}, the Cs_2TiI_6-based Perovskite solar cell device performs at its best. In this simulation based work the Power Conversion Efficiency (%), Fill Factor (%), Open-circuit Voltage (VOC) and Current Density (Jsc) have been investigated and found maximum efficiency of greater than 21.84 % when the absorber layer thickness is 4µm for optimized perovskite solar cell. This article's application of various technical techniques to increase the capacity of the absorbing materials to absorb photon energy has a wide range of applications. Perovskite solar cells have gained a lot of interest in recent years due to the advantages they offer over other forms of solar cells. In terms of their power conversion efficiencies (PCEs), perovskite solar cells have outperformed a number of other types of solar cells. It's critical to remember that despite the fact that perovskite solar cells offer a lot of potential, challenges still need to be overcome. For instance, they need to scale up their production methods and increase their long-term stability and toughness. To overcome these challenges and reach the full potential of perovskite solar cells in a range of applications, work is still being done in research and development.

References

[1] M. A. Halim, M. M. Hossain and M. J. Nahar, “Development of a Nonlinear Harvesting Mechanism from Wide Band Vibrations,” *International Journal of Robotics and Control Systems*, 2(3), 467-476, 2022.

[2] Z. Akkuly *et al.*, "Optimization of the Solution-Based Aluminium Gallium Oxide Buffer Layer for CdTe Solar Cells," *2021 IEEE 48th Photovoltaic Specialists Conference (PVSC)*, Fort Lauderdale, FL, USA, 2021, pp. 2132-2135, doi: 10.1109/PVSC43889.2021.9519067.

[3] Y. S. Lee, et al., “Atomic layer deposited gallium oxide buffer layer enables 1.2 v open-circuit voltage,” in cuprous oxide solar cells Advanced Materials, vol. 26, pp. 4704–4710, 2019.

[4] Y. Zhang, Y. Yu, F. Meng and Z. Liu, "Experimental Investigation of the Shading and Mismatch Effects on the Performance of Bifacial Photovoltaic Modules," in *IEEE Journal of Photovoltaics*, vol. 10, no. 1, pp. 296-305, Jan. 2020, doi: 10.1109/JPHOTOV.2019.2949766..

[5] M. Sebai, I. Trabelsi, G. Bousselmi, J. L. Lazzari and M. Kanzari, "Growth and characterization of Cu2ZnxFe1-xSnS4 thin films deposited on n-type silicon substrates," *Physica B: Condensed Matter*, p. 414670, 2023.

[6] D-J. Xue, et al., "GeSe thin-film solar cells fabricated by self-regulated rapid thermal sublimation," Journal of the American Chemical Society, vol. 139, pp. 958–965, 2017, https://doi.org/10.1021/jacs.6b11705.

[7] M. A. Halim, S. K. Biswas, M. S. Islam and M. M. Ahmed, "Numerical Simulation of Non-toxic ZnSe Buffer Layer to Enhance Sb2S3 Solar Cell Efficiency Using SCAPS-1D Software," *International Journal of Robotics and Control Systems*, vol. 2, no. 4, pp. 709-720, 2022.

[8] K. K. Maurya and V. N. Singh, "Enhancing the Performance of an Sb2Se3-Based Solar Cell by Dual Buffer Layer," *Sustainability*, vo. 13, no. 21, p. 12320, 2021.

[9] A. Das, D. Acharjee, M. K. Panda, A. B. Mahato and S. Ghosh, "Dodecahedron CsPbBr3 Perovskite Nanocrystals Enable Facile Harvesting of Hot Electrons and Holes," *The Journal of Physical Chemistry Letters*, 14, 3953-3960, 2023.

[10] D. K. Maram, H. Habibiyan, H. Ghafoorifard and O. Shekoofa, "Analysis of Optimum Copper Oxide Hole Transporting Layer for Perovskite Solar Cells," *2019 27th Iranian Conference on Electrical Engineering (ICEE)*, Yazd, Iran, 2019, pp. 214-219, doi: 10.1109/IranianCEE.2019.8786599.

[11] S. C. Ramesh, P. Ramkumar, C. C. Columbus and X. S. Shajan, "Experimental and Simulation Studies of Platinum-Free Counter Electrode Material for Titania Aerogel-Based Quasi-Solid Dye-Sensitized Solar Cell," in *IEEE Journal of Photovoltaics*, vol. 10, no. 6, pp. 1757-1761, Nov. 2020, doi: 10.1109/JPHOTOV.2020.3025693.

[12] M. Nicolescu*et al*., "Structural, Optical, and Sensing Properties of Nb-Doped ITO Thin Films Deposited by the Sol–Gel Method" *Gels*, vol. 8, no. 11, p. 717, 2022.

[13] S. A. Moiz, S. A., Albadwani and M. S. Alshaikh, "Towards Highly Efficient Cesium Titanium Halide Based Lead-Free Double Perovskites Solar Cell by Optimizing the Interface Layers," *Nanomaterials*, vol. 12, no. 19, p. 3435, 2022.

[14] K. Chakraborty and S. Paul, "Comparison of spectral responses of Cs2TiI6-XBrX based Perovskite device with CdS and TiO2 Electron transport layer," *In IOP Conference Series: Materials Science and Engineering*, vol. 1080, no. 1, p. 012007, 2021.

[15] H. Li *et al*., "Applications of vacuum vapor deposition for perovskite solar cells: A progress review," in *iEnergy*, vol. 1, no. 4, pp. 434-452, December 2022, doi: 10.23919/IEN.2022.0053..

[16] S. S. Hussain *et al*., "Numerical modeling and optimization of lead-free hybrid double perovskite solar cell by using SCAPS-1D," *Journal of Renewable Energy*, vol. 2021, pp. 1-12, 2021.

[17] H. Chen, H. Yi, B. Jiang, K. Zhang and Z. Chen, "Data-Driven Detection of Hot Spots in Photovoltaic Energy Systems," in *IEEE Transactions on Systems, Man, and Cybernetics: Systems*, vol. 49, no. 8, pp. 1731-1738, Aug. 2019, doi: 10.1109/TSMC.2019.2896922.

[18] X. Quan *et al*., "Photovoltaic Synchronous Generator: Architecture and Control Strategy for a Grid-Forming PV Energy System," in *IEEE Journal of Emerging and Selected Topics in Power Electronics*, vol. 8, no. 2, pp. 936-948, June 2020, doi: 10.1109/JESTPE.2019.2953178.

[19] M. Chen et al., "Cesium titanium (IV) bromide thin films based sTable leadfree perovskite solar cells," *Joule*, vol. 23, no. 3, pp. 558–570, 2018.

[20] S. Ahmed, F. Jannat, M. A. K. Khan, and M. A. Alim, "Numerical development of eco-friendly Cs2TiBr6 based perovskite solar cell with all-inorganic charge transport materials via SCAPS-1D," *Optik*, vol. 225, pp. 1–13, 2021.

[21] K. Chakraborty, M. G. Choudhury and S. Paul, "Life Cycle Assessment of a Lead-Free Cesium Titanium (IV) Single and Mixed Halide Perovskite Solar Cell Based 1 m² PV Module," in *IEEE Transactions on Device and Materials Reliability*, vol. 21, no. 4, pp. 465-471, Dec. 2021, doi: 10.1109/TDMR.2021.3106340.

[22] S. Ahmed, F. Jannat and M. A. Alim, "A study of Cesium Titanium Bromide based perovskite solar cell with different Hole and Electron transport materials," *2020 2nd International Conference on Advanced Information and Communication Technology (ICAICT)*, Dhaka, Bangladesh, 2020, pp. 297-301, doi: 10.1109/ICAICT51780.2020.9333520.

[23] C. Duan, Z. Zhao and L. Yuan, "Lead-Free Cesium-Containing Halide Perovskite and Its Application in Solar Cells," in *IEEE Journal of Photovoltaics*, vol. 11, no. 5, pp. 1126-1135, Sept. 2021, doi: 10.1109/JPHOTOV.2021.3095457.

[24] J. Siekmann, S. Ravishankar and T. Kirchartz, "Apparent defect densities in halide perovskite thin films and single crystals," *ACS Energy Letters*, vol. 6, no. 9, pp. 3244-3251, 2021.

[25] Li, Q. Z, M. Ni and X. D. Feng, "Simulation of the Sb2Se3 solar cell with a hole transport layer," *Materials Research Express*, vol. 7, no. 1, p. 016416, 2020.

[26] A. Shongalova *et al*., "Growth of Sb2Se3 thin films by selenization of RF sputtered binary precursors," *Solar Energy Materials and Solar Cells*, vol. 187, pp. 219-226, 2018.

[27] Y. Zeng, F. Liu, M. Green and X. Hao, "Fabrication of Sb2S3 planar thin film solar cells with closed-space sublimation method," *2018 IEEE 7th World Conference on Photovoltaic Energy Conversion (WCPEC) (A Joint Conference of 45th IEEE PVSC, 28th PVSEC & 34th EU PVSEC)*, Waikoloa, HI, USA, 2018, pp. 0870-0872, doi: 10.1109/PVSC.2018.8547305.

[28] S. Aseena, N. Abraham and V. S. Babu, "Optimization of layer thickness of ZnO based perovskite solar cells using SCAPS 1D," *Materials Today: Proceedings*, vol. 43, pp. 3432-3437, 2021.

[29] S. S. Joshi, "Solar Induced CO2 Reduction Achieved by Halide Tuning in Cesium Titanium (IV) Mixed Perovskite," *2021 IEEE 21st International Conference on Nanotechnology (NANO)*, Montreal, QC, Canada, 2021, pp. 299-302, doi: 10.1109/NANO51122.2021.9514279.

[30] S. A. Moiz, A. N. M. Alahmadi and A. J. Aljohani, "Design of a Novel Lead-Free Perovskite Solar Cell for 17.83% Efficiency," in *IEEE Access*, vol. 9, pp. 54254-54263, 2021, doi: 10.1109/ACCESS.2021.3070112..

[31] J. -H. Wi *et al*., "Spectral Response of CuGaSe2/Cu(In,Ga)Se2 Monolithic Tandem Solar Cell With Open-Circuit Voltage Over 1 V," in *IEEE Journal of Photovoltaics*, vol. 8, no. 3, pp. 840-848, May 2018, doi: 10.1109/JPHOTOV.2018.2799168..

[32] S. Srivastava, R. Walia, M. S. Chauhan, R. S. Singh and V. K. Singh, " Numerical investigation of silicon heterojunction solar cell with zinc selenide as electron-selective and nickel oxide as hole-selective contacts," *Optical Materials*, vol. 127, p. 112328, 2022.

[33] R. Parasuraman and K. Rathnakannan, "Al/n-ZnO /n+MoS2/p-Si/Ag Heterojunction Solar Cell Based on Pyro-Piezo-Photovoltaics Effect," *2019 IEEE 1st International Conference on Energy, Systems and Information Processing (ICESIP)*, Chennai, India, 2019, pp. 1-4, doi: 10.1109/ICESIP46348.2019.8938365.

[34] C. Gobbo *et al*., "Effect of the ZnSnO/AZO Interface on the Charge Extraction in Cd-Free Kesterite Solar Cells," *Energies*, vol. 16, no. 10, p. 4137, 2023.